Q. J. R. Meteorol. Soc. (2004), **130**, pp. 2377–2390 doi: 10.1256/qj.03.120

Aircraft observations of cloud droplet number concentration: Implications for climate studies

By I. GULTEPE* and G. A. ISAAC

Cloud Physics and Severe Weather Research Division, Meteorological Service of Canada, Toronto, Canada

(Received 11 July 2003; revised 29 April 2004)

SUMMARY

Droplet number concentration (N_d) is a major parameter affecting cloud physical processes and cloud optical characteristics. In most climate models, N_d is usually assumed to be constant or a function of the droplet and aerosol number concentration (N_a). Three types of cloud systems over Canada, namely Arctic clouds, maritime boundary-layer clouds, and winter storms, were studied to obtain values of N_d as a function of temperature (T). The probability density function of N_d was also calculated to show the variability of this parameter. The results show that N_d reaches a maximum at about 10 °C (200 cm^{-3}) and then decreases gradually to a minimum (∼1–3 cm^{-3}) at about −35 °C. A comparison of relationships between N_d and N_a indicates that estimates of N_d from N_a can have an uncertainty of about 30–50 cm^{-3}, resulting in up to a 42% uncertainty in cloud short-wave radiative forcing. This study concludes that the typical fixed values of N_d, which are ∼100 cm^{-3} and ∼200 cm^{-3} for maritime and continental clouds, respectively, and the present relationships of N_d to N_a, could result in a large uncertainty in the heat and moisture budgets of the earth's atmosphere. It is suggested that the use of relationships between N_d and T can improve climate simulations.

KEYWORDS: Climate change Droplet and aerosol number concentrations

1. INTRODUCTION

Changes in cloud microphysical parameters depend on thermodynamical and dynamical conditions, and aerosol–cloud interactions. Small changes in the particle size, shape, concentration, and mass can affect incoming and outgoing radiation, and this leads to significant changes in the earth–atmosphere energy budget, which result in a large uncertainty in climate simulations (Gultepe and Isaac 1996; Randall *et al.* 1998; Gultepe and Isaac 2002). Slingo (1990) stated that the top-of-the-atmosphere radiative forcing by doubled carbon dioxide can be balanced by increases of 15–20% in the amount of low clouds and 20–35% in liquid-water path, and by decreases of approximately 15–20% in mean drop radius. More recently, Rotstayn (1999a,b) used a global climate model to study the indirect radiative forcing due to modifications in liquid cloud properties. He found that indirect radiative forcing of about −2.1 W m^{-2} results from a 1% increase in cloudiness, a 6% increase in liquid water path, and a 7% decrease in effective radius. Knyazikhin *et al.* (2002) stated that the weakest link in the current radiative transfer models is the handling of cloud particle distribution. For example, a particle size distribution described in a cumulative way, rather than using a single particle size, may lead to increased cloud absorption. This suggests that a fixed value of droplet concentration, N_d, which is often used in model simulations, can cause a large uncertainty in climate simulations. All of the above references indicate that the uncertainty in N_d computed from empirical relationships is important and should be considered for climate-sensitivity studies.

The estimates of aerosol indirect forcing due to increasing aerosols (Penner *et al.* 2001) include increases in N_d associated with changes in cloud albedo (first indirect effect) and an increase in precipitation efficiency leading to decreased cloud amounts (second indirect effect). As stated by Penner *et al.* (2001), the uncertainty in the calculation of the indirect aerosol forcing (from −1.1 to −4.8 W m^{-2}) is relatively

* Corresponding author: Cloud Physics and Severe Weather Research Division, Meteorological Service of Canada, 4905 Dufferin St., Toronto, Ontario M3H-5T4, Canada. e-mail: ismail.gultepe@ec.gc.ca

large, and considerable effort is required to quantify its effects on climate change. Incorrect cloud fields, as might be simulated with poorly known N_d, impact a number of parameters, including air temperature (T), cloud water condensate and turbulent heat flux, which, in turn, could alter precipitation processes (Wetzel and Bates 1995).

Brenguier *et al.* (2000) studied a plane-parallel model for the parametrization of clouds in global climate models to estimate the effect of the vertical profile of microphysical parameters on radiative transfer calculations for boundary-layer clouds. Using cloud radiance measurements and assuming adiabatic conditions, retrieved N_d values were underestimated as compared to measured N_d. They suggested further analysis is needed. In their work, they also suggested that cloud optical thickness is proportional to the $5/3$ power of the cloud physical thickness and the $1/3$ power of N_d. They concluded that a very high accuracy of N_d is not required for the following reasons: (i) N_d is naturally very variable within the clouds; (ii) the indirect effect is sensitive to the cube root of N_d; and (iii) the expected change in N_d due to pollution is a factor of two to ten. Their work suggested that cloud radiative properties are particularly sensitive to cloud physical thickness and liquid water path.

The droplet effective radius (r_{eff}) is a function of N_d, and is also related to: cloud physical thickness, breadth of the particle spectra, liquid water content (LWC), and the available cloud condensation nuclei (Martin *et al.* 1994; Wood and Field 2000). When clouds become convectively active, microphysical parameters are influenced by vertical air motion. Increased vertical motions can result in larger droplets due to higher supersaturation values, and consequently r_{eff} becomes larger and N_d smaller because of coalescence. This suggests that stratiform clouds with embedded cells (Gultepe *et al.* 2000) may have smaller N_d compared to clouds without cells. It is not well known how turbulence affects the development of particle spectra, but a study by Kato *et al.* (2001) suggests that increased turbulent motions might also result in large droplets (large effective sizes) and fewer small droplets.

In this study, values of N_d, obtained from *in situ* measurements collected during three field projects (the Alliance Icing Research Study (AIRS), the Radiation Aerosols and Climate Experiment (RACE), and the First International Regional Experiment Arctic Cloud Experiment (FIRE.ACE)), were analysed to show the relationship between N_d and T, and then the probability density function (PDF) of N_d was calculated to signify the variability in N_d. The results are then compared with those of earlier studies. Finally, the use of N_d in climate simulations is discussed and conclusions given.

2. Observations

The *in situ* observations used in the analysis were collected using instruments mounted on the National Research Council Convair-580 aircraft during RACE (Gultepe *et al.* 1996), FIRE.ACE (Gultepe and Isaac 2002), and AIRS (Isaac *et al.* 2001) field campaigns; these took place over the Bay of Fundy and Central Ontario during August 1995, over the Arctic Ocean during April 1998, and over the Ontario region during the winter of 1999–2000, respectively. The observations collected during RACE, FIRE.ACE, and AIRS represent midlatitude summer clouds, Arctic clouds, and midlatitude winter clouds. The vast majority of the clouds sampled were stratiform. Measurements were made at 1 s intervals and the typical aircraft true air speed was approximately 85 m s^{-1}.

The 1 s average observations of LWC and total water content (TWC), N_d, aerosol number concentration (N_a) and T are used to derive relationships between N_d and T and between N_d and N_a. LWC and N_d are obtained from hot-wire probes (Nevzorov and

King probes) and Particle Measuring Systems (PMS) Forward Scattering Spectrometer Probes (FSSP), respectively. Under most circumstances, the Nevzorov probe LWC and TWC measurements are accurate to 10–15% (Korolev *et al.* 1998). The FSSP-100 probes had size ranges of either 3–45 or 5–95 μm. Uncertainties in LWC and N_d can be about 15% and 30%, respectively (Baumgardner *et al.* 1990). During FIRE.ACE and AIRS, N_a was obtained using a PMS Passive Cavity Aerosol Spectrometer Probe (PCASP), with a size range of 0.13–3 μm. During RACE, N_a measurements were obtained from a PMS Active Scattering Aerosol Spectrometer Probe (ASASP) over a size range from 0.17 to 2.0 μm. The air temperature was measured by a reverse flow temperature probe with an accuracy of ± 1 degC. A Rosemount icing detector and the Nevzorov LWC/TWC probe were used to segregate regions with supercooled liquid water from glaciated regions (Cober *et al.* 2001).

3. Analysis and results

A parametrization of N_d versus T can be used in climate models to estimate effective size (Gultepe *et al.* 2002). For this purpose, N_d was averaged over 5 degC intervals, and a best fit was obtained to the mean values for the entire dataset, including AIRS, RACE, and FIRE.ACE. In this work, only liquid segments were considered in the analysis, and mixed phase conditions were eliminated using the Rosemount icing detector and hot-wire probes. The clouds were defined as segments along which $N_d > 0.1$ cm^{-3} and LWC > 0.005 g m^{-3}. Figure 1(a) shows the 1 s data of N_d versus T. The mean and 20, 50 and 80 percentile values of N_d gradually decrease with decreasing T. The percentile values and the 1 s data indicate that a large variability in N_d exists, and this should be considered for future climate studies. The importance of N_d variability in climate studies was also stated by Brenguier *et al.* (2000). It is possible that the 20% and 80% values of N_d, can be used to represent variability in climate simulations. The equation for the best fit in Fig. 1(a) is:

$$N_d = -0.071T^2 + 2.213T + 141.56. \quad (1)$$

Gultepe and Isaac (1997) found similar trends in LWC, with LWC decreasing with decreasing T in stratiform clouds.

In Fig. 1(b), N_a versus T for cloud-free regions is shown. In order to obtain cloud-free regions, TWC < 0.001 g m^{-3} and N_d for standard size ranges <0.1 cm^{-3} are used, because the PCASP and ASASP measurements were significantly affected by cloud particles (Gultepe and Isaac 2002). The N_a values clearly decreased at low temperatures for both FIRE.ACE and AIRS. Large values of N_a are found for T greater than about $-10\,^{\circ}$C, where large values of N_d are also observed. Since colder temperatures are usually found at higher altitudes, this trend of N_a with temperature may also indicate the variability with height. Isaac *et al.* (1998), using similar instrumentation, found that aerosol concentrations often decrease with height.

The PDFs of the N_d parameter were also determined for AIRS, RACE, and FIRE.ACE field programmes, representing winter mixed-phase clouds, summer stratiform clouds, and Arctic boundary-layer clouds, respectively, because PDFs are commonly used in modelling studies. The seven standard types of PDF were used to quantify the PDF type for each field project. The PDF types are shown in Table 1. The mean and standard deviation (sd) values for N_d from each field programme, as well as related parameters such as skewness, were estimated using 1 s observations. The observed and estimated PDFs were then compared to conclude which type of PDF could be used to represent the N_d distributions (see Fig. 2).

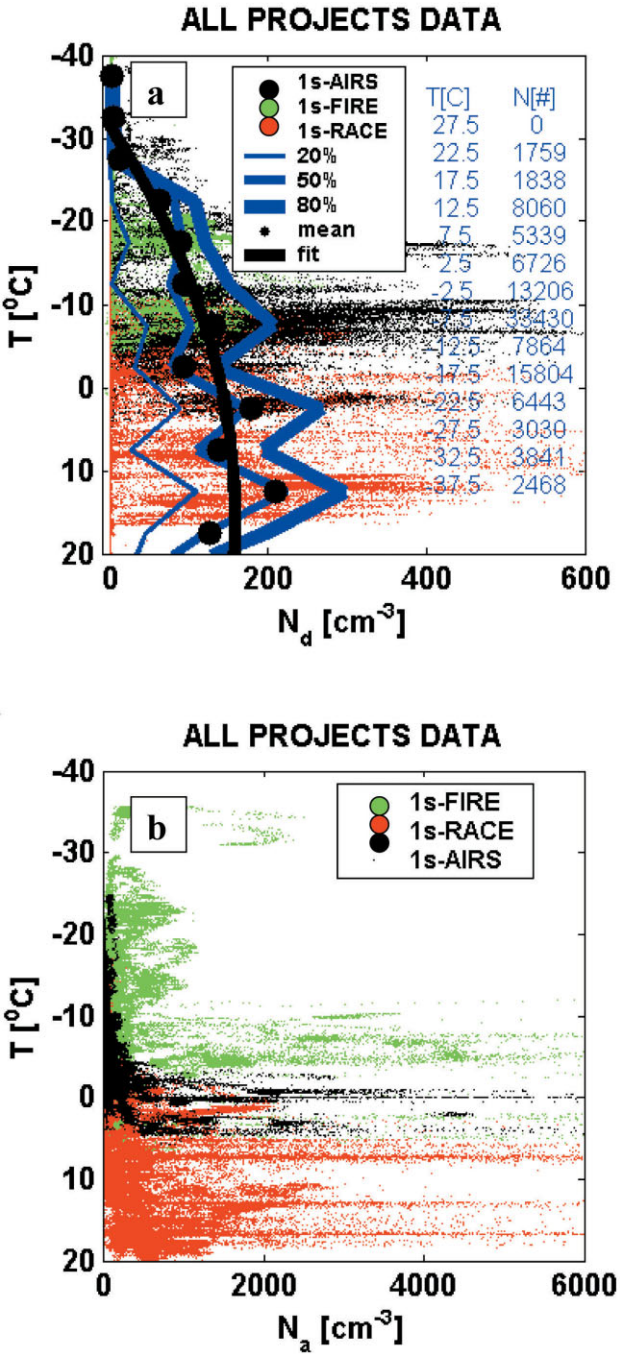

Figure 1. (a) Droplet number concentration (N_d) versus temperature (T); mean and percentiles together with a fit line, and the number of points (#) used in N_d measurements at 5 degC intervals are also shown. (b) Aerosol number concentration (N_a) versus T for cloud-free regions. From the three field projects AIRS, FIRE and RACE (see text for details).

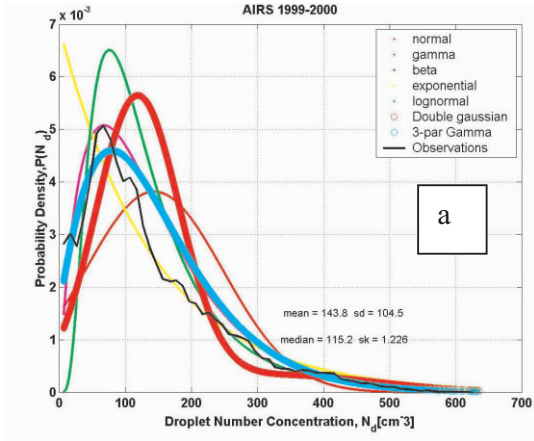

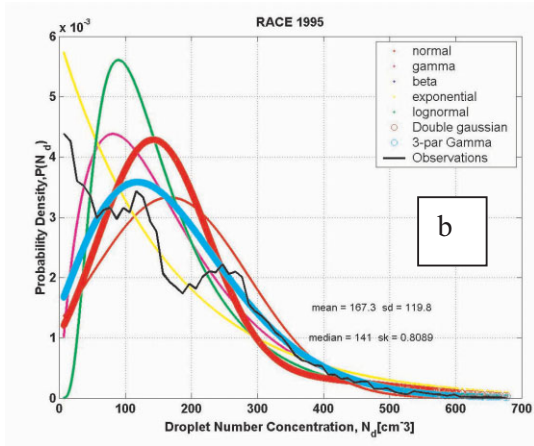

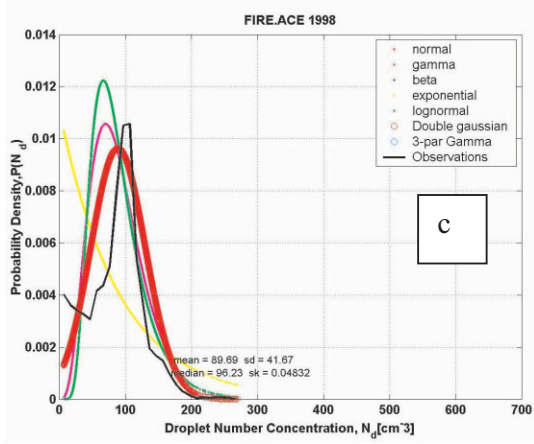

Figure 2. Probability density function (PDF) of droplet number concentration (N_d) observations for the field projects: (a) AIRS, (b) RACE, and (c) FIRE.ACE discussed in the text. The seven types of PDFs are shown along with the measured PDF. Values of each mean, standard deviation (sd), median and skewness (sk) are also given.

TABLE 1. THE VARIOUS PROBABILITY DENSITY FUNCTION FORMULAE USED IN DROPLET NUMBER (N_d) ESTIMATION

Distribution function	Probability density function formula	Parameter	Related parameters	Related parameters	Comments
Normal (Gaussian)	$f(x) = \frac{1}{\sigma\sqrt{2\pi}} \exp\left\{-\frac{(x-\mu)^2}{2\sigma^2}\right\}$	μ, σ			μ is the mean, σ is the standard deviation
Lognormal	$f(x) = \frac{1}{x\sigma_l\sqrt{2\pi}} \exp\left\{-\frac{(\ln(x)-\mu_l)^2}{2\sigma_l^2}\right\}$	μ, σ	$u_l = \frac{1}{2}\ln\left(\frac{\mu^4}{\mu^2+\sigma^2}\right)$	$\sigma_l = \sqrt{\ln\left(\frac{\sigma^2+\mu^2}{\mu^2}\right)}$	
Gamma (2-parameter)	$f(x) = \frac{1}{\beta^\alpha \Gamma(\alpha)} x^{\alpha-1} \exp\left(-\frac{x}{\beta}\right)$	α, β	$\beta = \frac{\sigma^2}{\mu}$	$\alpha = \frac{\mu}{\beta}$	Γ is the gamma function, β is a parameter
Gamma (3-parameter)	$f(x) = \frac{\lambda^M}{\Gamma(M)} \lvert x-x_o\rvert^{M-1} \exp\{-\lambda\lvert x-x_o\rvert\}$	M, λ, x_o	$M = \frac{4}{Sk^2}$ $\lambda = \frac{\sqrt{M}}{\sigma}$	$x_o = \overline{x} - \frac{2\sigma}{Sk}$	Sk is the skewness
Beta (2-parameter)	$f(x) = \frac{1}{\beta(\alpha,b)} x^{\alpha-1}(1-x)^{b-1}\mathrm{I}(0,1)(x)$	α, b, β	$\alpha = \frac{1-\mu-(\sigma/\mu)^2\mu}{(\sigma/\mu)^2} > 0$	$b = \left(\frac{1-\mu}{\mu}\right)\alpha > 0$	β is the Beta function
LWFGVC (Double Gaussian)	$f(s) = \frac{\alpha}{\sqrt{2\pi}\sigma_1} \exp\left\{-\frac{1}{2}\left(\frac{s-s_1}{\sigma_1}\right)^2\right\} + \frac{1-\alpha}{\sqrt{2\pi}\sigma_2} \exp\left\{-\frac{1}{2}\left(\frac{s-s_2}{\sigma_2}\right)^2\right\}$				Lewellen and Yoh (1993)
Exponential	$f(x) = \frac{1}{\mu} \exp\left(-\frac{x}{\mu}\right)$	μ			

One significant difference between data from these three field projects is that the mean (median) values of N_d were not constant, they ranged from: 144 (115) cm^{-3} for AIRS (Fig. 2(a)); 167 (<10) cm^{-3} for RACE (Fig. 2(b)); and 90 (96) cm^{-3} for FIRE.ACE (Fig. 2(c)). The most important point in comparing the PDFs from the three field programmes is that the PDF shapes are significantly different. This can partly be due to the effect of temperature, as shown in Fig. 1. For example, the cloud temperature during FIRE.ACE was generally the lowest (−35 to 0 °C) and the temperature in RACE clouds was generally the highest (−10 to 15 °C) of the three projects (Fig. 1(a)). When the temperature is low, there is usually less available moisture and dynamical forcing is reduced. This leads to less cloud condensation nuclei being activated and thus a reduced N_d. The observed differences in the PDFs indicate that assuming only one spectral shape for N_d within a General Circulation Model (GCM) and for remote sensing studies can result in large uncertainties in the derived parameters.

The PDFs for AIRS (Fig. 2(a)) and RACE (Fig. 2(b)) are best represented with a gamma distribution as:

$$PDF(N_d) = \frac{1}{b^a \Gamma(a)} x^{a-1} \exp\left(-\frac{x}{b}\right), \tag{2}$$

where the mean (144 cm^{-3}) and variance (105 cm^{-3}) of the data for AIRS are equal to axb and axb^2. For RACE, PDF(N_d) is an exponential distribution (Fig. 2(b)), which is a simple form of the gamma distribution with $a = 1$ and $b =$ mean (167 cm^{-3}). For FIRE.ACE, the distribution is represented by a Gaussian PDF (Lewellen and Yoh 1993) (Fig. 2(c)). When the skewness vanishes (∼0; as in this case), the double Gaussian PDF is reduced to a single Gaussian distribution in which mean and sd are directly obtained from the data. The mean concentration difference between the fitted PDFs for the gamma and Gaussian distributions is found to be about 25–30 cm^{-3}; this can be significant for climate studies.

4. Discussion

Radiative transfer models (Hunt 1973; Hansen and Travis 1974; Stephens and Tsay 1990) and remote sensing retrievals (Liu et al. 2003) use a modified gamma size distribution for cloud studies as:

$$n(r) = cr^{(1-3b)/b} \exp\{-r/(ab)\}, \tag{3}$$

where c is the normalization constant obtained as:

$$c = N_{dt}(ab)^{(2b-1)/b} / \Gamma\{(1-2b)/b\}, \tag{4}$$

where $n(r)$ is the particle number density. The total number concentration, N_{dt}, is usually assumed to be constant in the calculations (Hunt 1973; Menon *et al.* 2002); Γ is the gamma function, $a = r_{eff}$, and b is the effective variance, v_{eff}, which is assumed to be 0.193 for stratiform clouds (Stephens and Tsay 1990) and depends on cloud type. It can be written that $n(r) = f(N_{dt}, r_{eff}, v_{eff})$ and the uncertainty in $n(r)$ is related to N_{dt}. Figure 3 shows $n(r)$ versus r for various N_{dt} ranging from 50 up to 500 cm^{-3} with $r_{eff} = 10$ (15) μm and $v_{eff} = 0.20$ (0.10), representing stratus (cumulus) clouds. This plot shows that $n(r)$ is strongly related to N_{dt}, and its values need to be accurately determined for various cloud systems.

Establishing the dependency of N_d on N_a is limited by uncertainties in measurements of both parameters, also the limited datasets and the analysis techniques used for

various cloud types. Detailed analyses of N_d versus N_a by Gultepe and Isaac (1996, 1999) were obtained using 20 km averages. Figure 4, obtained from both works, suggests that variability in the data was significant, and there was no unique relationship between N_d and N_a. Martin *et al*. (1994) and Leaitch *et al*. (1996) analysed the N_d and N_a data using averages over the entire cloud leg, and Leaitch *et al.* summarized the results for only sulphate particles. Differences in the two investigations may be due to their analysis techniques. If the Martin *et al* (1994) equations are combined, as in Jones *et al*. (1994), the difference between values of N_d (Fig. 4) can be as large as 60 cm^{-3}, which can result in about a 40% change in short-wave (SW) cloud-forcing (CF) values (see discussion following Eq. (13)).

The effect of uncertainties in N_d on cloud albedo (A) can be estimated using a relationship between optical thickness and cloud physical characteristics (Platnick and Twomey 1994):

$$\tau_{ext} = \pi Q_{ext} \left\{ \frac{LWC}{\rho_w (4/3)\pi} \right\}^{2/3} N_d^{1/3} \Delta z, \tag{5}$$

where Q_{ext} is the Mie efficiency factor assumed to be approximately 2 for large particles at the visible and near-infrared radiation; Δz is the cloud physical thickness, and ρ_w is water density. Based on Eq. (5), τ_{ext} is related to the 1/3 power of N_d. The effect of N_d on calculations of τ_{ext} can also be obtained from the following definition of extinction parameters:

$$\sigma_{ext} = \pi Q_{ext}(x) N_d r_s^2, \tag{6}$$

(Hansen and Travis 1974) where particle mean surface radius, r_s, and N_d are directly related to σ_{ext}. Using $k = r_v^3/r_{eff}^3$ (r_v is the mean volume radius) and $r_{eff} = r_v^3/r_s^2$ (Brenguier *et al.* 2000):

$$\sigma_{ext} = \pi k Q_{ext}(x) N_d r_{eff}^2. \tag{7}$$

This shows that if we multiply both sides by Δz, we get the optical thickness as

$$\tau_{ext} = \pi k Q_{ext}(x) N_d r_{eff}^2 \Delta z, \tag{8}$$

where τ_{ext} is directly related to first power of N_d in contrast to the 1/3 power of N_d in Eq. (5). Equation (8) shows that Eq. (5) is not a unique equation to correlate τ_{ext} with N_d. However, using simple, but approximate relationships between r_{eff}, N_d and LWC, Eqs. (5) and (8) can be shown to very similar. If we take a natural logarithm given by the formula $d(\ln x) = dx/x$, assuming only N_d and r_{eff} are variables, Eq. (8) becomes:

$$\frac{d\tau_{ext}}{\tau_{ext}} = \frac{dN_d}{N_d} + 2\frac{dr_{eff}}{r_{eff}}, \tag{9}$$

and by neglecting nonlinear terms in the Taylor series (Mandel 1984), Eq. (6) is written as:

$$\frac{\Delta\tau_{ext}}{\tau_{ext}} = \frac{\Delta N_d}{N_d} + 2\frac{\Delta r_{eff}}{r_{eff}}. \tag{10}$$

Then, assuming $\tau_{ext} = 5$, $N_d = 100$ cm^{-3}, $r_{eff} = 10$ μm, and applying a 10% change in both r_{eff} (1 μm) and N_d (10 cm^{-3}), $\Delta\tau_{ext}$ is estimated to be about 1.5, resulting in a 30% uncertainty in τ_{ext}.

Using Eq. (5) and assuming a conservative scattering in the cloud, the two-stream approximation results in an albedo–optical-thickness relationship (Hansen and Travis 1974; Lacis and Hansen 1974; Platnick and Twomey 1994) as

$$A \cong \{\sqrt{3}(1-g)\tau_{ext}\}\{2 + \sqrt{3}(1-g)\tau_{ext}\}, \tag{11}$$

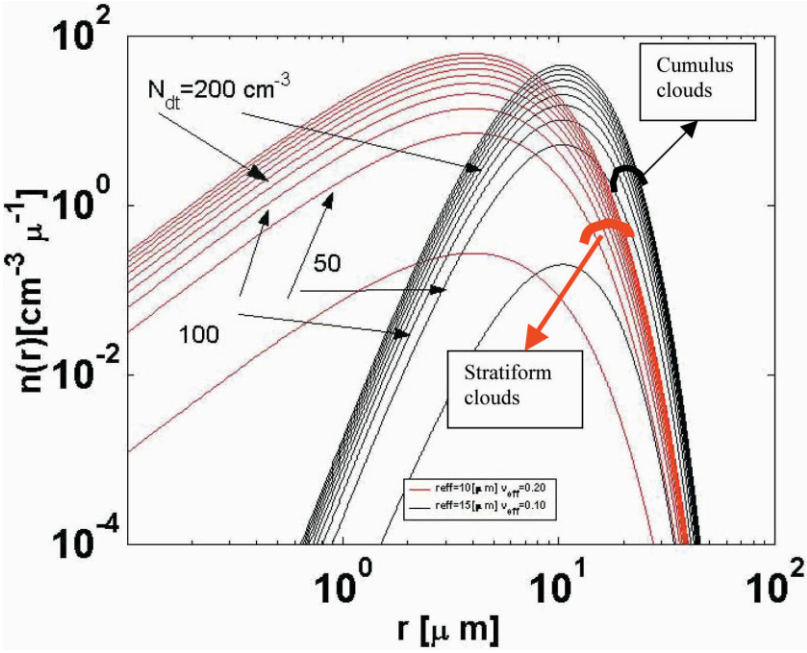

Figure 3. A modified gamma size distribution for various values of droplet effective radius (r_{eff}), effective variance (v_{eff}), and total number concentration (N_{dt}) that are used in calculation of the value of constant c in Eq. (4).

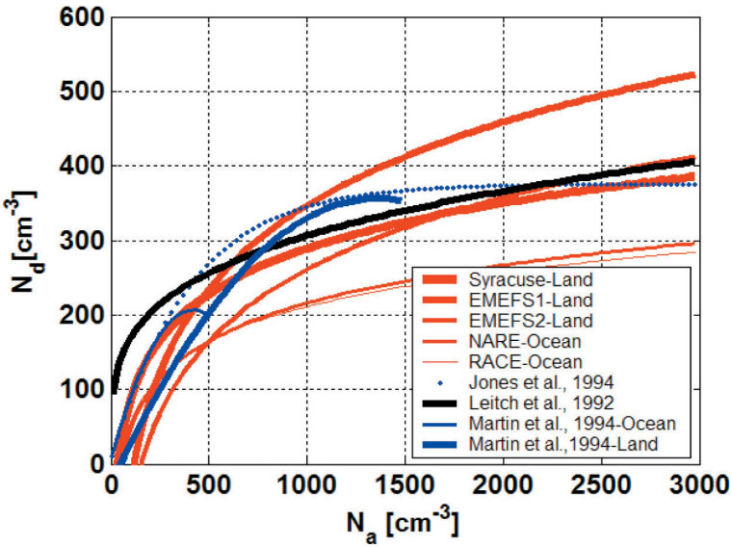

Figure 4. The relationships between droplet number concentration (N_{d}) and aerosol number concentration (N_{a}) obtained from observations given in Gultepe and Isaac (1996, 1999) and from other works.

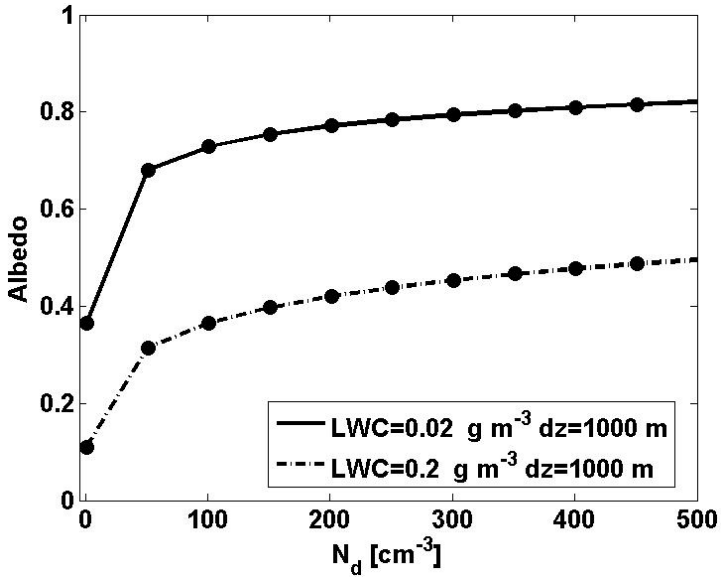

Figure 5. Cloud planetary albedo (A) versus droplet number concentration (N_d) for two values of liquid water content (LWC) assuming a cloud physical thickness of 1000 m.

where g is the asymmetry factor, which for simplicity is assumed to be 0.85 for liquid clouds but in reality it is a function of particle size. The mean values for N_d used in some GCMs range from 60 up to 600 cm^{-3} (Table 2). The use of mean values greater than 200 cm^{-3} for GCMs can result in overestimation of planetary albedo (Fig. 5). Figure 5 shows cloud planetary albedo versus N_d calculated using Eqs. (5) and (11), where LWC is assumed constant at either 0.2 or 0.02 g m^{-3} within a 1000 m cloud layer. It is also clear that for small values of N_d ($<$100 cm^{-3}), A changes more than for the same amount of change in large N_d values. A small change in N_d, for either large or small values of N_d, can be important for calculations of the heat budget. It should be noted that changes in N_d are not only important for radiative effects but also for physical processes and precipitation conversion processes.

Using LWC $= 0.02$ g m^{-3} and $\Delta z = 1$ km for a typical boundary-layer non-precipitating liquid cloud layer, τ_{ext} is calculated for two values of N_d (100 and 150 cm^{-3}). The corresponding values of A change from approximately 0.35 to 0.40, indicating that a 15% change in A occurs for a 50% change in N_d (Fig. 5). Using the values of $A_{100} = 0.35$ ($N_d = 100$ cm^{-3}) and $A_{150} = 0.40$ ($N_d = 150$ cm^{-3}), and assuming the planetary albedo for clear sky (A_{cl}) is 0.30 and the mean solar constant (S_0) is about 1380 W m^{-2} (Wallace and Hobbs 1977), the respective SW radiative cloud forcings (Sohn and Robertson 1993) for $N_d = 100$ cm^{-3} and $N_d = 150$ cm^{-3} are estimated from:

$$CF_{100} = S_0(A_{100} - A_{cl}), \tag{12}$$

and

$$CF_{150} = S_0(A_{150} - A_{cl}). \tag{13}$$

Then, $(CF_{150} - CF_{100})/CF_{100}$ becomes 40%, indicating that a 50% change in N_d can result in a 40% change in SW CF. This value can increase or decrease depending on the N_d values used in Eq. (5). A summary of the column average of T values from models and observations from the Atmospheric Radiation Measurement site indicated

TABLE 2. DROPLET NUMBER CONCENTRATION (N_d) VALUES USED IN GCM STUDIES AND RESULTS FROM THE PRESENT WORK

Reference	Model type or Observations	N_d (cm^{-3})	Condition
Lee *et al.* 1997	NCAR CCM2[1]	150	Ocean
		600	Land
Ghan *et al.* 1999	NCAR CCM2[1]	100	Both
Del Genio *et al.* 1996	GISS[2]	60	Ocean
		170	Land
Rotstayn 1999a	CSIRO[3] GCM	100	Ocean
		500	Land
Present work	Data type	Mean (Median)	Cloud type
AIRS	*In situ*	144(115)	Winter storms
FIRE.ACE	*In situ*	90(96)	Arctic boundary-layer clouds
RACE	*In situ*	167(141)	Marine boundary-layer clouds

[1]National Center for Atmospheric Research Community Climate Model.
[2]Goddard Institute for Space Studies.
[3]Commonwealth Scientific and Industrial Research Organization.
For other acronyms see text.

that the difference in temperature between observations and single-column models can be as high as 10 degC, showing that the representation of clouds in the climate models needs to be improved (Ackerman and Stokes 2003).

5. CONCLUSIONS

The following conclusions related to characteristics of N_d have been reached:

(i) When N_d was held constant in GCMs (Table 2), the values in different models for clouds over oceans ranged from 60 to 150 cm^{-3}, while the values over land ranged from 100 to 600 cm^{-3}. Thus there is no unique value to be used in GCMs for N_d.

(ii) N_{dt}, currently used as a constant value in gamma size distributions, cannot be fixed because N_d is found to be related to T and this can affect SW cloud forcing. For example, a 50% change in N_d from 100 to 150 cm^{-3} can result in a change of approximately 40% in SW forcing.

(iii) Various analysis methods used in the relationships between N_d and N_a complicate the accurate estimation of N_d. In some GCMs, N_d is related to sulphate particle concentration (Penner *et al.* 2001); however, such particles may only represent 30–40% of the total mass of particles, consequently this technique can also lead to an underestimation of N_d.

(iv) The PDFs obtained from the present work indicate that N_d sizes can be represented by a gamma, exponential, or normal distribution, and mean values were found to be significantly different for each cloud system. A gamma size distribution is not unique for all datasets. These variations can be due to environmental and cloud physical–dynamical conditions that affect the particle size distribution.

(v) The use of N_d PDFs for polluted and clear environments in climate studies can reduce the uncertainty that may arise due to the relationships between N_d and N_a currently used, or they can be compared with model outputs to better understand microphysics–climate interactions.

(vi) The results also indicate that relationships between τ_{ext} and N_d (Eqs. (5) and (8)) are not unique. A 30% change in τ_{ext} (Eq. (8)) can be caused by a 10% change in N_d (near 100 cm^{-3}) and a 10% change in r_{eff} (near 10 μm) when cloud physical thickness is fixed. The r_{eff} contribution to the 30% change in optical thickness is twice the N_d contribution.

The above conclusions indicate that there are many difficulties in the representation of liquid clouds within climate models. We need to develop better methods for determining N_d. Certainly using constant values over land or ocean cannot accurately represent nature. The use of a single PDF is also open to question because there are many variables, such as T, that can affect N_d.

ACKNOWLEDGEMENTS

The Panel on Energy Research and Development and NASA Langley provided financial support for FIRE.ACE. The National Search and Rescue Secretariat of Canada, Boeing Commercial Airplane Group, Transport Canada, and the Department of National Defense provided funding for the AIRS project. The aircraft data were obtained using the National Research Council of Canada Convair-580 and the scientific and technical efforts of many National Research Council and Meteorological Service of Canada staff. The authors thank J. W. Strapp for discussions related to the data analysis.

REFERENCES

Ackerman, T. P. and Stokes G. M. 2003 The atmospheric radiation measurement program. *Phys. Today.*, **56**(1), 38–43

Baumgardner, D., Cooper, W. A. and Dye J. E. 1990 *Optical and electronic limitations of the forward scattering spectrometer probe: Liquid particle size measurement techniques*. Vol. 2, ASTM STP 1083. Eds. E. Dan Hirleman, W. D. Bachalo and P. G. Felton. American Society for Testing and Materials, Philadelphia, USA

Brenguier, J. L., Pawlowska, H., Schuller, L., Preusker, R., Fischer, J. and Fouquart, Y. 2000 Radiative properties of boundary layer clouds: Droplet effective radius versus number concentration. *J. Atmos. Sci.*, **57,** 803–821

Cober, S. G., Isaac, G. A., Korolev, A. V. and Strapp J. W. 2001 Assessing cloud-phase conditions. *J. Appl. Meteorol.*, **40,** 1967–1983

Del Genio, A. D., Yao, M.-S., Kovari, W. and Lo, K. K.-W. 1996 A prognostic cloud water parameterization for global climate models. *J. Climate*, **9,** 270–304

Ghan, S. J., Leung, L. R. and McCaa, J. 1999 A comparison of three different modeling strategies for evaluating cloud and radiation parameterizations. *Mon. Weather Rev.*, **127,** 1967–1984

Gultepe, I., and Isaac, G. A. 1996 The relationship between cloud droplet and aerosol number concentrations for climate models. *Int. J. Climatol.*, **16,** 1–6

1997 Relationship between liquid water content and temperature based on aircraft observations and its applicability to GCMs. *J. Climate*, **10,** 446–452

1999 Scale effects on averaging of cloud droplet and aerosol number concentrations: Observations and models. *J. Climate*, **12,** 1268–1279

2002 The effects of air-mass origin on Arctic cloud microphysical parameters during FIRE.ACE. *J. Geophys. Res.*, **107**(C10), SHE 4–1 to 4–12

Gultepe, I., Isaac, G. A., Leaitch, W. R. and Banic, C. 1996 Parameterizations of marine stratus microphysics based on *in-situ* observations: Implications for GCMs. *J. Climate*, **9,** 345–357

Gultepe, I., Isaac, G., Hudak, D., Nissen, R. and Strapp, W. 2000 Dynamical and microphysical characteristics of arctic clouds during BASE. *J. Climate*, **13,** 1225–1254

Gultepe, I., Isaac, G. A. and Cober, S. G. 2002 Cloud microphysical characteristics versus temperature for three Canadian field projects. *Annales Geophysica*, **20**(11), 1891–1898

Hansen, J. E. and Travis, L. D. 1974 Light scattering in planetary atmospheres. *Space Sci. Rev.*, **16,** 527–610

Hunt, G. E. 1973 Radiative properties of terrestrial clouds at visible and infrared thermal window wavelengths. *Q. J. R. Meteorol. Soc.*, **99,** 346–369

Isaac, G. A., Banic, C. M., Leaitch, W. R., Anlauf, K. G., Couture, M. D., Liu, P. S. K., Macdonald, A. M., MacQuarrie, K. I. A., Puckett, K. J. and Wiebe, H. A. 1998 Vertical profiles and horizontal transport of atmospheric aerosols and trace gases over central Ontario. *J. Geophys. Res.*, **103,** 22015–22037

Isaac, G. A., Cober, S. G., Strapp, J. W., Korolev, A. V., Tremblay, A. and Marcotte, D. L. 2001 Recent Canadian research on aircraft in-flight icing. *Can. Aeronaut. Space J.*, **47,** 213–221

Jones, A., Roberts, D. L. and Slingo, A. 1994 A climate model study of indirect radiative forcing by anthropogenic sulphate aerosols. *Nature*, **370,** 450–453

Kato, S., Mace, G. G., Clothiaux, E. E., Liljegren, J. C. and Austin, R. T. 2001 Doppler radar derived size distributions in liquid water stratus clouds. *J. Atmos. Sci.*, **58,** 2895–2911

Knyazikhin, Y., Marshak, A., Wiscombe, W. J., Martonchik, J. V. and Myneni, R. B. 2002 A missing solution to the transport equation and its effect on estimation of cloud absorptive properties. *J. Atmos. Sci.*, **59,** 3572–3585

Korolev, A. V., Strapp, J. W., Isaac, G. A. and Nevzorov, A. 1998 The Nevzorov airborne hot wire LWC/TWC probe: Principles of operation and performance characteristics. *J. Atmos. Oceanic. Technol.*, **15,** 1496–1511

Lacis, A. A. and Hansen, J. E. 1974 A parameterization for the absorption of solar radiation in the earth's atmosphere. *J. Atmos. Sci.*, **31,** 118–133

Leaitch , W. R., Isaac, G. A., Strapp, J. W., Banic, C. M. and Wiebe, H. A. 1992 The relationship between cloud droplet concentrations and anthropogenic pollution: Observations and climatic implications. *J. Geophy. Res.*, **97,** 2463–2474

Leaitch, W. R., Banic, C. M., Isaac, G. A., Couture, M. D., Liu, P. S. K., Gultepe, I., Li S.-M., Kleinman L. I., Daum, P. H. and MacPherson J. I. 1996 Physical and chemical observations in marine stratus during the 1993 North Atlantic Regional Experiment: Factors controlling cloud droplet number concentrations. *J. Geophys. Res.*, **101**(D22)**,** 29123–29135

Lee, W.-H, Iacobellis, S. F. and Somerville, R. C. J. 1997 Cloud radiation forcings and feedbacks: General circulation model tests and observational validation. *J. Climate*, **10,** 2479–2496

Lewellen, W. S. and Yoh, S. 1993 Binormal model of ensemble partial cloudiness. *J. Atmos. Sci.*, **50,** 1228–1237

Liu, G., Shao, H., Coakley, J. A., Curry, J. A., Haggerty, J. A. and Tschudi, M. A. 2003 Retrieval of cloud droplet size from visible and microwave radiometric measurements during INDOEX: Implication to aerosols' indirect effect. *J. Geophys. Res.*, **108**(D1)**,** 4006, AAC 2-1 to AAC 2-10

Mandel, J. 1984 *The statistical analysis of experimental data.* Dover Publications Inc., New York, USA

Martin, G. M., Johnson, D. W. and Spice, A. 1994 The measurement and parameterization of effective radius of droplets in warm stratocumulus clouds. *J. Atmos. Sci.*, **51,** 1823–1842

Menon, S., Delgenio, A. D., Koch, D. and Tselioudis, G. 2002 GCM simulations of the aerosol indirect effect: Sensitivity to cloud parameterization and aerosol burden. *J. Atmos. Sci.*, **59,** 692–713

Penner, J. E., Andrae, M., Annegarn, H., Barrie, L., Feichter, J., Hegg, D., Jayaraman, A., Leaitch, R., Murphy, D., Nganga, J., Pitari, G., Ackerman, A., Adams, P., Austin, P., Boers, R., Boucher, O., Chin, M., Chuang, C., Collins, B., Cooke, W., DeMott, P., Feng, Y., Fisher, H., Fung, I., Ghan, S., Ginoux, P., Gong, S.-L., Guenther, A., Herzog, M., Higurashi, A., Kaufman, Y., Kettle, A., Kiehl, J., Koch, D., Lammel, G., Land, C., Lohmann, U., Madronich, S., Mancini, E., Mishchenko, M., Nakajima, T., Quinn, P., Rasch, P., Roberts, D. L., Savoie, D., Schwartz, S., Seinfield, J., Soden, B., Tanre, D., Taylor, K., Tegen, I., Tie, X., Vali., G., Van Dingenen, R., Weele, M. V. and Zang, Y. 2001 'Aerosols, their direct and indirect effects, a chapter in Climate Change 2001'. Pp. 289–348 in *Contributions of Working Group I to the Third Assessment Report of the Intergovernmental Panel on Climate Change*. Cambridge University Press, New York, USA

Platnick, S. and Twomey, S. 1994 Determining the susceptibility of cloud albedo to changes in droplet concentration with the advanced very high-resolution radiometer. *J. Appl. Meteorol.*, **33,** 334–347

Randall, D., Curry, J., Battisti, D., Flato, G., Grumbine R., Hakkinen, S., Martinson, D., Preller, R., Walsh, J. and Weatherly, J. 1998 Status of and outlook for large-scale modeling of atmosphere–ice–ocean interactions in the Arctic. *Bull. Am. Meteorol. Soc.*, **79,** 197–209

Rotstayn, L. D. 1999a Climate sensitivity of the CSIRO GCM: Effect of cloud modeling assumptions. *J. Climate*, **12,** 334–356

1999b Indirect forcing by anthropogenic aerosols: A global climate model calculation of the effective-radius and cloud-lifetime effects. *J. Geophys, Res.*, **104,** 9369–9380

Slingo, A. 1990 Sensitivity of the earth's radiation budget to changes in low clouds. *Nature*, **343,** 49–51

Sohn, B-J, and Robertson, F. R. 1993 Intercomparison of observed cloud radiative forcing: A zonal and global perspective. *Bull. Am. Meteorol. Soc.*, **74,** 997–1006

Stephens, G. L. and Tsay, S.-C. 1990 On the cloud absorption anomaly. *Q. J. R. Meteorol. Soc.*, **116,** 671–704

Wallace, J. M. and Hobbs, P. V. 1977 *Atmospheric science: An introductory survey*. Academic Press Inc., Orlando, USA

Wetzel, M. A. and Bates, G. T. 1995 Comparison of simulated cloud cover with satellite observations over the western United States. *J. Climate*, **8,** 296–314

Wood, R. and Field, P. R. 2000 Relationships between total water, condensed water, and cloud fraction in stratiform clouds examined using aircraft data. *J. Atmos. Sci.*, **57,** 1888–1905